Published in final edited form as:
Pharm Res. 2012 September ; 29(9): 2587–2600. doi:10.1007/s11095-012-0789-2.

Dermal microdialysis technique to evaluate the trafficking of surface modified lipid nanoparticles upon topical application

Pinaki R. Desai[1], **Punit P. Shah**[1], **Ram R. Patlolla**[2], and **Mandip Singh**[1,*]

[1]College of Pharmacy and Pharmaceutical Sciences, Florida A&M University; Tallahassee, FL 32307, USA

[2]Dr. Reddys Laboratories, Integrated Product Development, Bachupallyi, Hyderabad, AP 500090, India

Abstract

Purpose—The central objective of the current study was to evaluate the skin pharmacokinetics and tissue distribution of cell penetrating peptides (CPP) modified nano-structured lipid carrier (NLC) using an in vivo dermal microdialysis (MD) technique.

Methods—Celecoxib (Cxb) encapsulated NLCs (CXBN), CPP modified CXBN (CXBN-CPP) and Cxb-Solution (CXBS) formulations were prepared and tested for in vitro skin distribution. MD was used to assess pharmacokinetic parameters of Cxb after topical application of Cxb formulations. The effect of pre-treatment with Cxb formulations was evaluated for expression of prostaglandin-E2 (PGE_2) and Interleukin-6 (IL-6) after exposure of xylene using MD. Allergic contact dermatitis (ACD) model was used to confirm in vivo therapeutic response of Cxb formulations.

Results—The cumulative permeation of Cxb in MD dialysate after 24 h for CXBN-CPP was significantly higher ($p<0.001$) than CXBN and CXBS. Further, pre-treatment with CXBN-CPP significantly inhibited PGE_2 and IL-6 expression compared to CXBS and CXBN ($p<0.001$). In ACD model, CXBN-CPP showed significant reduction ($p<0.001$) in ear thickness compared to controls.

Conclusions—Surface modification of NLC with CPPs can enhance the skin permeation of Cxb and MD can be used to investigate pharmacokinetics of Cxb nanoparticles in the skin.

Keywords

Nanoparticles; Dermal Pharmacokinetics; Cell Penetrating Peptides; Microdialysis; Polyarginine peptide

INTRODUCTION

Topical treatment of the skin diseases appears to be effective and favorable treatment because of the lower risk of the systemic effects. However, the stratum corneum (SC) counteracts the penetration of active drugs into the viable skin. One way of optimizing topical drug delivery to the skin is the use of nanocarriers. During the last decade, an unmeasured number of research papers have been published describing the use of nanostructured lipid carriers (NLC) for the topical application mainly due to their ability to improve penetration across SC and for their targeting properties (1-2). However, NLCs can't

[*]**Corresponding Author:** Mandip Singh, College of Pharmacy and Pharmaceutical Sciences, Florida A & M University, Tallahassee, FL 32307. Tel: (850) 561-2790; Fax: (850) 599-3813. mandip.sachdeva@gmail.com.

permeate into the deep skin layers. Thus, in order to improve the permeation of active drug into the deeper skin layers, our laboratory has already shown that the surface modification of NLCs with trans-acting activator of transcription (TAT) peptide has an ability to deliver encapsulated drug molecule into the lower epidermis and dermis which is the site of most skin diseases (3-4). It was proposed that the translocation efficiency of cell penetrating peptides (CPPs) is mainly due to the cationic residues of these peptides. More importantly, it was suggested that nonamer (9-mer) arginine peptides (R_9) have more translocation capabilities compared to other cationic amino acids such as histidine, lysine and ornithine (5). In addition, the effect of the number of arginine (R_n; n=4 to 16) residues in the CPPs is studied for their translocation effects into the cells (6-7). These studies suggested that R_4 has extremely low, while R_6 and R_8 have maximum and R_{16} has less translocation activity. On the other hand, the effect of the polyarginine chain length on the skin delivery of cargo molecules particularly nanocarriers is still unexplored. Therefore in this study we have examined the effects of the polyarginine chain length on the skin delivery of NLC by selecting polyarginine-8 (R_8), polyarginine-11 (R_{11}) and polyarginine-15 (R_{15}) in comparison with a well known CPP like TAT and non-transducing peptide, YKA (YKALRISRKLAK).

Furthermore, the in vivo release of drugs in the deeper skin layers from topically applied NLC is still unknown and unexplored. Also, an investigation of pharmacokinetic profile of dermatological formulations is a challenge to the pharmaceutical scientists. Since dermatological drug products are designed to target the local tissue to which they are applied, the amount of drug reaching to systemic circulation is very small. Therefore, the general procedure used for evaluation of pharmacokinetics of orally administered drug products is not suitable for topical products. An in vitro technique uses Franz diffusion set up for determining availability of a drug in the different skin layers. However, this technique has limitations like i) lack of elimination phase in terms of the vascular system and viable metabolizing enzymes and ii) alteration in the SC structure due to water uptake. Therefore an in vivo technique is necessary to obtain the clinically relevant information about the pharmacokinetics of drug in the skin and to investigate the pharmacological response of the drug. Very few techniques are available that allows direct assessment of drug concentrations in the dermis (8). These techniques include the skin blister-fluid method and biopsy followed by tissue homogenization. However, ethical considerations and cost limit the applicability of these techniques in evaluating pharmacokinetics of a topical formulation. Also, these techniques can't be used to evaluate the therapeutic response. Therefore, to overcome these limitations, dermal microdialysis (MD) can be used as an in vivo technique for investigation of pharmacokinetic and therapeutic response of a drug in the skin (8-10).

MD sampling has been introduced and developed to study the dermal drug levels after topical drug application on animals including rodents and humans (11). The method consists of placing an ultrathin semipermeable hollow fiber structure in the dermis (epidermal-dermal junction) and perfusing this fiber, called a probe, with a tissue-compatible buffer at a very low rate by means of microdialysis pump. The probe functions as an artificial vessel in the dermis and thus exchanges small and diffusible molecules between the outside tissue space and the perfusion fluid according to law of diffusion (12). The recovery of the drug of interest closely reflects the concentration of unbound (pharmacologically active) drug in the intracellular fluid of the tissue surrounding the probe (13). This results in the concentration-time profile which can be useful in determining the pharmacokinetics of a drug in the skin. Further MD has been used to evaluate the skin penetration of topical formulations (14) like gels, creams, ointments and lotions. However, the use of MD still unexplored for evaluation of the skin penetration of nanoparticles. Therefore, MD was selected and used as a valuable in vivo tool to evaluate dermal pharmacokinetic profiles and to quantify the drug release from the NLCs and CPP modified NLCs (NLC-CPP). Celecoxib (Cxb), a non-steroidal anti-

inflammatory drug (NSAID), was selected as our model drug since Cxb has many appropriate characteristics for topical application such as: low molecular weight (381.37 (g/mol)), high stability, no skin irritant properties, high lipophilicity (Log P value - 3.5) and most importantly, it is selective cyclo-oxygenase-2 (COX-2) inhibitor, used for pain management.

MD can also be used to evaluate endogenous substances or to study the mechanism of physiological and pathological tissue events in normal, damaged or diseased skin. It is well documented that dermal MD allows real-time measurement of inflammatory mediators in the dermis of normal as well as diseased skin (15). Being selective COX-2 inhibitor, Cxb suppresses prostanoid production involved in pain and inflammation (16). Furthermore, IL-6 is a multifunctional cytokine produced in skin damage like inflammatory conditions and plays a central role in modulating immunity (17). Therefore we have examined the effect of pre-treatment of Cxb containing formulations on the expression of prostaglandin E2 (PGE_2) and IL-6 levels after application of xylene, an irritant chemical which is among the 30 most abundantly produced chemicals in the United States and is also found in petroleum mixtures (18).

To study the effect of CPP modified NLCs on the Cxb delivery into the skin, specific aims of the current study were to: 1) prepare and characterize CPP modified NLCs; 2) study the effects of arginine chain length on the in vitro skin permeation of Cxb using hairless rat skin as a model; 3) evaluate the Cxb concentration at the epidermal-dermal junction for NLCs and NLC-CPP using MD; 4) assess the effect of NLCs and NLC-CPP pre-treatment followed by exposure to xylene on the expression of PGE_2 and IL-6 biomarkers by dermal MD and 5) investigate the therapeutic response of NLC-CPP in an in vivo inflammatory mouse model of allergic contact dermatitis (ACD).

MATERIALS AND METHODS

Materials

Celecoxib (Cxb) was a generous gift from Pfizer (Skokie, IL). The triglyceride Miglyol 812 and Compritol 888 ATO were kind gift samples from Sasol Germany GmbH (Witten, Germany) and Gattefosse (Saint Priest, France). 1,2-dioleoyl-*sn*-glycero-3-[(*N*-(5-amino-1-carboxypentyl) imidodiacetic acid) succinyl nickel salt] (DOGS-NTA-Ni) was purchased from Avanti polar lipids (Alabaster, AL, USA). Tetrahydrofuran, tween 80 and xylene were procured from Sigma-Aldrich Chemicals (St. Louis, USA). Polyoxyethylene-20 oleyl ether (Volpo-20) was a kind gift from Croda Inc (Edison, NJ, USA). Vivaspin centrifuge filters (Molecular weight Cut off: 10, 000 Daltons) were procured from Sartorius Ltd, (Stonehouse, UK). All the histidine tagged peptides TAT (YGRKKRRQRRRHHHHHH, MW: 2382.67); Polyarginine-8 (RRRRRRRRHHHHHH, MW: 2203.54); Polyarginine-11 (RRRRRRRRRRHHHHHH, MW: 2672.21); Polyarginine-15 (RRRRRRRRRRRRRRHHHHHH, MW: 3296.86); and Non-transduction peptide YKA (YKALRISRKLAKHHHHHH, MW: 2269.7) were synthesized by CHI Scientific, Inc (Maynard, MA, USA). Enzyme immunoassay (EIA) kits for rat IL-6 and PGE_2 were purchased from Pierce Biotechnology Inc (Thermo Scientific, Rockford, IL, USA) and R&D Systems (Minneapolis, MN, USA), respectively. All other chemicals used in this research were of analytical grade.

Animals—CD® (SD) hrBi hairless rats (350-400 g; male; Charles River Laboratories, Wilmington, MA) and C57BL/6 mice (6 weeks old; male; Charles River Laboratories, Wilmington, MA) were grouped and housed (n=6 per cage) in cages with bedding. The animals were kept under controlled conditions of 12:12 h light:dark cycle, 22 ± 2 °C and 50 ± 15% RH. The mice were fed (Harlan Teklad) and water ad libitum. The animals were

housed at Florida A&M University in accordance with the standards of the Guide for the Care and Use of Laboratory Animals and the Association for Assessment and Accreditation of Laboratory Animal Care (AAALAC). The animals were acclimatized to laboratory conditions for one week prior to experiments. All the animal protocols followed were approved by the Animal Care and Use Committee, Florida A & M University, FL.

Preparation of nano structured lipid carriers (NLCs)—NLCs containing Cxb, a model drug, (CXBN) were formulated by using hot melt high pressure homogenization technique (19). Briefly, two phases oil phase and aqueous phase were prepared and heated at 85 °C. The melted lipid phase containing Cxb (0.1% w/v), solid lipid (Compritol 7.0% w/v), oil (Miglyol 3.0% w/v), and DOGS-NTA-Ni (0.02% w/v) were dispersed in a hot aqueous surfactant solution (Tween 80 2.4% w/v) at 85 °C to produce a pre-emulsion by high speed stirring using a Virtis Cyclone IQ2 blade type homogenizer at 20,000 rpm for 1 min. This hot pre-emulsion was further processed by passing through Nanodebee® (South Easton, MA, USA), high-pressure homogenizer at 20,000 psi for 5-6 cycles. The surface of prepared CXBN was then modified by simply incubating NLCs with six histidine tagged CPPs (CXBN-CPP) and YKA (CXBN-YKA) at room temperature for 30 minutes.

Physicochemical characterization of lipid nanocarries

Particle size and zeta potential: The mean diameter and polydispersity index (PI) of NLCs were measured by using Nicomp 380 ZLS (Agilent Technologies, Santa Clara, CA, USA). The Nicomp 380 ZLS analyzer uses dynamic light scattering to obtain the essential features of the particle size distribution. The particle size analysis data was evaluated using volume distribution. Prior to the measurement, the samples were diluted with HPLC grade water to suitable scattering intensity. The zeta potential values of CPP and YKA modified and unmodified NLCs were assessed by determining the particle electrophoretic mobility using Nicomp 380 ZLS. Both measurements were performed in triplicate each time.

Assay and entrapment efficiency: The assay was performed to find the total amount (bound and unbound) of the Cxb present in CXBN. Briefly, 100 μl of the formulation was dissolved in 900 μl of tetrahydrofuran and the centrifuged at 13,000 rpm for 10 minutes. Final dilutions were made with acetonitrile and Cxb content was determined by high-performance liquid chromatography (HPLC). The entrapment efficiency of Cxb in the NLCs was determined by using vivaspin columns (3). The vivaspin columns with 10,000 Daltons molecular weight cut off membrane was selected for the current study. 500 μl of CXBN formulation was loaded in the membrane containing donor compartment of column followed centrifugation at 3,500 rpm for 10 minutes. The receiver fluid was analyzed with HPLC for free Cxb.

In vitro percutaneous permeation

Preparation of skin: For skin collection, CD (SD) hrBi hairless rats were sacrificed by an overdose of halothane anesthesia. The skin from the dorsal surface was excised, and then adherent subcutaneous fat and connective tissues were removed carefully. The storage conditions were previously optimized by our laboratory where the effect of different storage conditions on the permeation of melatonin and nimesulide by using cryoprotecting agent (CPA) were studied. We have observed that the incubation of skin in aqueous glycerol (a well-known CPA) followed by freezing at −22 °C can maintain the viability for longer periods (20). In addition, the report on guidelines on processing and clinical use of skin allografts mention that skin storage at −80 °C can provide the long term storage with the use of CPA (21). Therefore in the present study the skin was stored in 10% w/w glycerol in saline at −80 °C and used within a week. Prior to use, the skin was rinsed in PBS (pH 7.4) for 30 min.

In vitro permeation study: The skin was mounted on Franz diffusion cells (Permegear Inc., Riegelsville, PA) between the donor and receiver compartment with epidermis facing the donor compartment. 200 μl of surface modified and unmodified formulations CXBN, CXBN-TAT, CXBN-R_8, CXBN-R_{11}, CXBN-R_{15} and CXBN-YKA formulations were applied on the diffusional surface of the skin in the donor compartment. The receiver compartment was filled with PBS (pH 7.4) containing 0.1% volpo-20, stirred at 300 rpm and maintained at 32°C ± 0.5°C using a circulating water bath. For comparison, 1 mg/ml Cxb solution (CXBS) was prepared by dissolving known amount of Cxb in 10% v/v ethanol and 2.4% w/v tween 80 in polyethylene glycol (PEG 400) (3). Skin permeation studies were performed for 2, 6, 12 and 24 h under unocclusive conditions. The receiver fluid was collected at the end of the study and was further investigated for the amount of Cxb permeated in the receiver fluid. For the skin collection, after pre-determined time period, the donor cell was removed and the excess formulation was removed from the surface of the skin using a cotton swab. The excess amount of Cxb remaining on the skin surface and present in the donor compartments was also evaluated by HPLC. The skin was then washed with 50% v/v ethanol and blotted dry with lint-free absorbent wipes. The entire dosing area (0.636 cm^2) was collected with a biopsy punch. The collected skin was then used for further studies.

In vitro skin retention of celecoxib—Cxb formulation exposed skin was collected after pre-determined time points of 2, 4, 6, 12 and 24 h. Cryotome was used to separate all three layers of the skin SC, epidermis and dermis. The horizontal (lateral) sectioning was performed using cryotome. First two sections of 10 μm were collected to represent the SC. Next four sections of 25 μm thickness were collected to represent epidermis and the remaining portion represented the dermis. 250 μl of PBS (pH 7.4) was then added to all the collected skin sections and heated on boiling water bath. After 10 minutes, all the samples were cooled down to room temperature and then 250 μl of acetonitrile was added. The vials were sonicated in a bath sonicator for 30 seconds and then vortexed for 2 minutes. Finally, all the tissue samples were centrifuged at 13,000 rpm for 15 minutes. The supernatant was collected and the extracts were analyzed for Cxb content using HPLC.

Assessment of CPP modified nanoparticulate delivery of celecoxib using dermal microdialysis

In vitro evaluation of probe recovery: To characterize the transfer rate of the probes and to evaluate the possible binding effect of Cxb, in vitro recovery of Cxb was assessed. The standard stock solution of Cxb (100,000, 10,000 and 1000 pg/ml) was prepared in 0.5% (w/v) volpo-20 containing Krebs-Ringer solution (138mM NaCl, 5 mM KCl, 1 mM MgCl2, 1 mM CaCl2, 11 mM NaHCO3, 1 mM NaH2PO4). A linear MD probes containing 10 mm dialysis membrane (LM-10, Bioanalytical Systems, West Lafeyetter, IN, USA) were used for these studies. A LM-10 microdialysis probe (n=4) was placed in a 5 ml vial containing Cxb standard stock solutions under continuous agitation. The temperature of the vial was maintained at 37 ± 1 °C by placing the vial in a thermostatic water bath. The inlet end of the probe was connected to a microinjection pump (CMA/102, CMA microdialysis, North Chelmsford, MA, USA) with the help of tubing connector. The outlet was connected to microfraction collector (CMA/142, CMA microdialysis, North Chelmsford, MA, USA). The laboratory MD experimental set up with descriptive figure is reported in our prior publications (17-18). Prior to recovery experiments, dialysis probes were equilibrated by perfusing with 50% ethanol for 30 min, followed by deionized water for 15 min and finally with 0.5% (w/v) volpo-20 in Krebs-Ringer solution for 30 min. The probes were continuously perfused with 0.5% (w/v) volpo-20 in Krebs-Ringer solution at flow rates of 1, 2, 3 and 4 μl/min to optimize the flow rate of perfusate. Dialysate samples were collected every 60 min for 240 min. Cxb concentration was measured in the dialysate (Cout) along

with the concentration in the surrounding medium (Cm). The percent relative recovery was calculated by using the formula:

$$\text{Dialysate concentration (Cout)} \times 100/\text{standard stock concentration (Cm)} \quad \text{Equation 1}$$

In vivo evaluation of probe recovery: In vivo recovery of Cxb was determined by retrodialysis methods. CD (SD) hrBi hairless rats were anaesthetized with an intraperitoneal injection of urethane (1.5 g/kg) and placed on a temperature controlled heating pad (37 ± 1 °C). For dermal implantation of the LM-10 probe containing 10 mm dialysis, the skin of the dorsal region of the rat was punctured with 19-gauge intravenous needle (BD Company, Franklin Lakes, NJ, USA). The MD probe was inserted through the guiding needle cannula and the needle was then retracted leaving the dialysis membrane in the skin horizontally. The same MD setup was used and the probe was equilibrated as explained in the section of in vitro evaluation of probe recovery. Cxb standard stock in 0.5% (w/v) volpo-20 in Krebs-Ringer solution was passed through the probe using an infusion pump at flow rate of 2 μl/ml and dialysate samples were collected every 60 min for 480 min. The recovery was determined from the ratio of the concentration loss to the initial concentration in the perfusate:

$$\% \text{ Recovery} = [(\text{Perfusate concentration} - \text{Dialysate concentration}) / \text{Perfusate concentration}] \times 100 \quad \text{Equation 2}$$

In vivo skin microdialysis: The MD setup described earlier for recovery studies was used. Briefly, linear MD probes were used and were continuously perfused with 0.5% (w/v) volpo-20 in Krebs-Ringer solution at a flow rate of 2 μl/min. Dialysate samples were collected every hour into refrigerated micro-fraction collector throughout the study period. Two MD probes were implanted in parallel position on the dorsal surface of the rat skin. The needle was carefully inserted in the skin so that the needle can be visible through the superficial skin layer. Our laboratory has reported the effect of probe depths on the skin permeation of active drugs (17-18). Therefore to examine the probe depth, the rat was sacrificed at the end of the study and the full thickness sections of the collected skin were taken using cryotome and were observed with microscope. In any set up the depth of the probe was not greater than 350 ±17 μm which was in agreement with our previous findings (18). After insertion of a probe through needle, the skin undergoes a trauma. To recover from it, Cxb formulations were applied topically after 1 h from the removal of needle and insertion of a probe. For topical application of surface modified and unmodified nanocarriers, the donor chambers were fixed on the rat skin at the point where MD membranes were implanted using crazy glue. 200 μl of CXBS, CXBN, CXBN-R_{11} and CXBN-YKA (n=4) were applied on the skin surface using donor chambers. Subsequently MD samples were collected every hour for 24 h and the dialysate samples were analyzed for Cxb levels using HPLC. The area under time vs. concentration curve (AUC) was calculated using the trapezoidal method. Further, maximum Cxb concentration in the dialysate at time‘t’ (Tmax) was considered as Cmax.

Efficacy of modified celecoxib-NLC to control release of proinflammatory biomarkers of skin irritation by dermal microdialysis

In vitro evaluation of probe recovery: To evaluate the transfer rate of the probes and to evaluate the possible binding effect of PGE_2 and IL-6 with the probes, in vitro recovery of PGE_2 and IL-6 was assessed as described by Patlolla et al with modifications (17). Briefly, to assess the recovery rate of PGE_2, LM-10 microdialysis probe was placed in a 5 ml vial containing 1000 pg/ml stock solution prepared in Krebs-Ringer solution. The probe was connected through the MD system as explained earlier. The equilibrated probe was perfused

with Krebs-Ringer solution at flow rates of 1, 2, 3 and 4 μl/min for 240 min. For the recovery of IL-6, equilibrated CMA 20 probe was placed in 2000 pg/ml IL-6 stock solution and perfused with 0.1% w/v BSA in Krebs-Ringer solution at flow rates of 0.5, 1 and 2 μl/min. The inflammatory biomarkers concentration in dialysate (Cout) and in the surrounding medium (Cm) was measured by using EIA kits as per manufacturer's instructions. The relative recovery was calculated using equation 1.

Effect of pre-treatment of CPP modified NLC: The same MD setup was used for these studies. In order to study the effect of modified and unmodified CXBN on the expression of PGE_2 and IL-6, the exposure site on the back of rat was pre-treated with 200 μl of CXBS, CXBN, CXBN-R_{11} and CXBN-YKA dispersion All the Cxb formulations were applied unocclusively 16 h prior to the probe insertion. Thereafter the formulations were wiped off five times using cotton balls, soaked in 50% v/v ethanol solution. The probe was then inserted at the exposure sites and baseline perfusate was collected for first 2 h.

Occlusive dermal exposure of xylene was carried out by using Hill top chambers® for 2 h (18). Following dermal exposures, dialysate samples were collected every hour for 5 h and stored at −80 °C till analysis. As a control, unloaded Hill top chambers® were placed on the skin above the MD probe and removed at the same time as treatment to study the skin chamber induced inflammatory effect. All the above procedures were performed under urethane anesthesia.

Analysis of celecoxib using HPLC in skin layers and microdialysates—The HPLC analysis of Cxb was performed with minor modifications from a reported method (22). Briefly, HPLC system was comprised of an auto sampler (model 717 plus), binary pump (model 1525), Waters UV photodiode array detector (model 996). The mobile phase consisting of acetonitrile, water, acetic acid (54:45:1% v/v) was pumped through the Symmetry C18 column (5 μm, 4.6 × 250 mm) at a flow rate of 1.0 ml/min and the eluent was monitored at 254 nm. The Cxb stock solution was prepared with acetonitrile and the serial working standard solutions were prepared in mobile phase. All injections were performed at room temperature.

In vivo model for allergic contact dermatitis (ACD)—C57BL/6 mice were sensitized on day zero by applying 25 μl of 0.5% v/v DNFB in acetone:olive oil (4:1) on the shaved abdomen. Mice were then challenged on day 5 by epicutaneous application of 25 μl of 0.2% DNFB in acetone:olive oil (4:1) on the right ear in order to induce an ACD response. The left ears were treated with vehicle alone (acetone:olive oil 4:1) and served as an internal control. The ACD response was determined by the degree of ear swelling compared with that of the vehicle treated contra-lateral ear before DNFB challenge. The increase in ear thickness was measured with a vernier caliper (Fraction+ Digital Fractional Caliper, General Tools & Instruments Co., LLC., New York, NY) at 0, 24, 48 and 72 h. Right ears of the mice were treated with topical applications of CXBS, CXBN, CXBN-R_{11} and CXBN-YKA, 2 h after antigen challenge and 3 times a day thereafter for 3 days. Dexamethasone, 0.5 mM solution in ethanol and PEG-400 mixture was used as a positive control. The ear swelling was measured before the application of Cxb formulations. This was considered as 0 h ear thickness. Then Cxb formulations like, CXBS, CXBN, CXBN-R_{11} and CXBN-YKA were applied and the ear thickness was measured at 24, 48, and 72 h. The ACD response was determined by taking a difference between 0 h and other time points. The mice ears were collected at the end of the study (72 h) and sectioned. These histological sections were observed after hematoxylin and eosin (H&E) staining with an optical microscope (Olympus America, Melville, NY).

Statistical Analysis—The Cxb content of the skin tissue was expressed as percent dose permeated. Differences between the skin permeation and microdialysate concentration of different Cxb formulations were examined using ANOVA and Tukey multiple comparison test. Mean differences with $p<0.001$ were considered to be significant.

RESULTS

Physicochemical characterization of lipid nanocarries

The prepared CXBN had particle size in the range of 120 nm - 150 nm with mean particle size of 134 ± 11 nm. The surface modification of NLCs with CPPs showed less effect on particle size. The mean diameter of the CXBN was increased from 134 ± 11 nm to 145 ± 15 nm. CXBN showed a narrow size distribution with PI of 0.15 ± 0.03. However, the zeta potential of prepared CXBN was highly affected by surface modification with CPPs. The zeta potential of the CXBN in double distilled water (pH 6.4) was found to be −19.78 mV, which increased to −7.84 mV after surface modification with CPP. Further, the zeta potential of the CXBN changed to −11.18 mV after surface modification with YKA. The prepared CXBN showed encapsulation efficiency of 95 - 97%. The total Cxb present in NLC dispersion was found to be 0.75 mg/ml. This assay value was used to calculate the percent entrapment and dose permeation.

In vitro permeation and retention of celecoxib

In order to assess the skin permeation and localization of Cxb, an in vitro skin permeation study was performed with CPP modified and unmodified NLCs. Cxb permeation from CPPs modified NLCs was significantly higher ($p<0.001$) at different collection points (2, 6, 12 and 24 h) compared to CXBS, CXBN and CXBN-YKA. However, the amount of Cxb in the receiver fluid was below the limit of detection by HPLC at the end of 24 h. The skin permeation profile of active drug depends on the physicochemical properties. This was demonstrated in our laboratory by performing skin permeation of a peptide, spantide II (MW – 1668, Log P – 6) and small molecule, ketoprofen (MW – 254, Log P – 3.1) from NLCs where ketoprofen was able to permeate across the skin. However spantide II was unable to permeate across the skin leading to increase in skin retention (23). The recovery from donor compartment was nearly 93-96 % of the applied dose. This can be partly explained by the high lipophilicity of the drug preventing diffusion from the skin into the receiver fluid. The comparative skin retention of drug from Cxb formulations is depicted in Figs. 1 to 4. After 2 h of skin permeation, Cxb from CPP modified and unmodified nanoparticle formulations started permeating into epidermis (Fig. 1). However, Cxb was not detected in the dermis till 6 h of skin permeation (Fig. 2). Further, the skin retention of Cxb increased dramatically into different skin layers from 12 h to 24 h of skin permeation (Figs. 3 and 4). Surface modification of CXBN with CPPs resulted in enhanced skin retention after 24 h compare to CXBS, CXBN and CXBN-YKA ($p<0.001$). Cxb permeation was increased with increase in arginine chain length from R_8 to R_{11} but further increase in arginine chain length resulted in decreased skin permeation. After 24 h of permeation, the percent of Cxb retained in dermis for CXBS, CXBN, CXBN-TAT, CXBN-R_8, CXBN-R_{11}, CXBN-R_{15} and CXBN-YKA was as follows: 0.123 ± 0.021, 0.464 ± 0.010, 0.991 ± 0.015, 0.793 ± 0.010, 1.534 ± 0.012, 1.168 ± 0.018 and 0.461 ± 0.028. At all time points the level of Cxb in different skin layers was significantly higher ($p<0.001$) for CXBN-R_{11} compared to other CPPs modified CXBN like: CXBN-TAT, CXBN-R_8 and CXBN-R_{15}.

In vivo CPP modified nanoparticulate delivery of celecoxib using dermal microdialysis

In vitro evaluation of probe recovery—The Cxb recovery from the LM-10 probe is summarized in Table I. The total recovery from the probe was dependent on the flow rate of the perfusion fluid. The slower flow rate showed effective recovery of the Cxb at the end of

240 min. The total percent recovery at the end of 240 min was 57.48 ± 0.76% to 45.16 ± 1.74% for the flow rates of 0.5 μl/min to 4 μl/min, respectively. However, when the flow rate was varied from 1 μl/min to 2 μl/min, the total recovery was not affected. Therefore, 2 μl/min of flow rate was selected for further studies to collect enough volume of dialysate to meet the 100 μl of injection volume in the HPLC.

In vivo evaluation of probe recovery—Data for in vivo recovery of LM-10 probe were determined by the retrodialysis method and are shown in Fig. 5. The average recovery of the Cxb over 480 min was 80.43% in the skin. The dialysis membrane showed steady loss of Cxb for 480 min through the LM-10 microdialysis probe.

In vivo skin microdialysis—Following topical application of CXBS, CXBN, CXBN-R_{11} and CXBN-YKA onto the intact hairless rat skin, no detectable concentration in the dialysate was found after 1 h of permeation. Cxb was able to permeate effectively from the skin to the dialysis membrane and was detected in the dialysate at end of 2 h. The change in Cxb concentration in the skin after 24 h for CXBS, CXBN, CXBN-R_{11} and CXBN-YKA is shown in Fig. 6. The skin absorption of Cxb from CXBS was rapid with Cmax value of 0.030 ± 0.0052 μg/ml at Tmax of 4 h which declined till 8 h and thereafter a steady concentration of the Cxb was observed. On the other hand, the Cmax for CXBN and CXBN-R_{11} was found to be 0.078 ± 0.0047 μg/ml at Tmax of 15 h and 0.16 ± 0.0096 μg/ml at Tmax of 13 h, respectively. Similarly, the Cmax for CXBN-YKA was found to be 0.095 ± 0.0063 μg/ml at Tmax of 14 h. This indicates that when Cxb was applied in the form of NLCs, it takes time to reach the maximum drug concentration in the deeper skin layers. The concentration vs. time profile showed that the levels of permeated Cxb were high for the NLCs and NLCs modified with CPPs at the end of 24 h. These results indicate that the permeation of Cxb from CXBN-R_{11} was significantly higher than CXBN, CXBN-YKA and CXBS ($p<0.001$) after 24 h. The $AUC_{0\text{-}24h}$ for Cxb was 0.541 ± 0.063, 1.345 ± 0.094, 2.714 ± 0.135 and 1.549 ± 0.075 μg×hr/ml from CXBS, CXBN, CXBN-R_{11} and CXBN-YKA, respectively. The total permeation of the Cxb from CXBN, CXBN-R_{11} and CXBN-YKA was increased by 2.5, 5.0 and 2.9 folds compare to CXBS, respectively.

In vivo efficacy of modified NLC to control release of proinflammatory biomarkers of skin irritation by dermal microdialysis

In vitro evaluation of probe recovery—For the in vitro recovery assessment of the probes, stock solution of 1000 pg/ml was selected, since the recovery of PGE_2 and IL-6 was less than 5% with 100,000 and 10,000 pg/ml of stock solution. The relative recovery for PGE_2 at 0.5 to 4 μl/min (n=4) was approximately 35% over a period of 240 min with no significant difference between the different flow rates (Table I). However, the recovery of IL-6 was influenced by the flow rate of the perfusion fluid. At lower flow rate (0.5 μl/min), the relative recovery was 16% versus 2% recovery at a flow rate of 4 μl/min. Therefore, flow rates of 2 μl/min and 0.5 μl/min were selected for PGE_2 and IL-6, respectively.

Effect of pre-treatment of CPP modified NLC—Occlusive dermal exposure of xylene resulted in release of PGE_2 and IL-6 which was determined using MD. For untreated control, insertion of needle into the rat skin showed release of inflammatory markers and the baseline values were achieved within 2 h after retrieval of the needle.

Xylene exposure resulted in a significant increase in PGE_2 levels after 1 and 2 h of exposure (Fig. 7). However, after removal of xylene, PGE_2 levels decreased at the end of 3 h. Pre-treatment of the skin with Cxb inhibited the xylene mediated increase in PGE_2. After pre-treatment with CXBN-R_{11}, the levels of PGE_2 were decreased and were found to be same as that of untreated control (Fig. 7). The levels of the PGE_2 were significantly less ($p<0.001$)

for CXBN-R_{11} treatment compared to xylene control, CXBS, CXBN and CXBN-YKA. This suggests that NLCs modified with R_{11} can deliver more amount of Cxb into the dermis to inhibit the release of PGE_2.

The linear probe failed to detect expression of IL-6 but CMA-20 probes effectively detected the IL-6 levels in the skin. Similar to PGE_2, IL-6 levels were decreased after 2 h of baseline period (untreated control). Fig. 8 shows the effect of pre-treatment of CXBS, CXBN, CXBN-R_{11} and CXBN-YKA on the release of IL-6 after the occlusive exposure of irritant chemical. Following application of xylene, IL-6 release was increased gradually and reached the maximum levels after removal of the xylene within 3 h. The expression levels for IL-6 were significantly less ($p<0.001$) for CXBN-R_{11} compared to CXBS, CXBN, CXBN-YKA. However, even after 5 h of removal of xylene, IL-6 levels were significantly more compared to PGE_2 for all the treatment groups.

In vivo model for allergic contact dermatitis (ACD)

The ACD model was developed as explained in (24-25). Briefly, the DNFB was applied on the right ears epicutaneously which resulted in the swelling and inflammation, while the left ear served as the internal standard without any swelling. Therefore, the effectiveness of different Cxb formulations to treat the inflammation was assessed by monitoring reduction in the ear swelling of the right ear. The ear thickness for all the controls and Cxb formulations after 24, 48 and 72 h of the treatment are summarized in the Fig. 9. After treatment with dexamethasone, the ear thickness was reduced significantly ($p<0.001$) compared to untreated control. CXBN-R_{11} demonstrated significant reduction ($p<0.001$) in ear swelling compared to CXBS, CXBN and CXBN-YKA. The ear thickness for CXBS, CXBN, CXBN-R_{11} and CXBN-YKA ($n=4$) was 56.26, 33.83, 15.25 and 32.50 μm, respectively, at the end of 72 h of treatment. These results suggest that ear thickness for CXBN-R_{11} was reduced by 3.7, 2.2 and 2.1 folds compared to CXBS, CXBN and CXBN-YKA, respectively.

The reduction of ear inflammation by R_{11} modified CXBN formulation was further characterized by cutaneous histological examination after 72 h of treatment. CXBN-R_{11} was highly effective in the treatment of ACD by the reduction of ear swelling as compared to untreated control, unmodified CXBN and CXBN-YKA treated ears (Fig 10).

DISCUSSION

Microdialysis has been considered a promising approach for the evaluation of drug pharmacokinetics and expression of biomarkers in the skin after topical application of dermatological drug products. Moreover, the in vivo pharmacokinetic profile of nanoparticles into the skin is unknown and needs to be investigated for understanding of free and active local drug concentrations at the damaged and/or diseased state of skin. In the present study, we have used dermal MD as a tool to investigate pharmacokinetic profile in the normal skin and expression of inflammatory biomarkers in the inflamed skin using polyarginine peptide modified NLCs.

For skin delivery purpose lipid nanocarriers are widely studied as they show adhesiveness, occlusion and skin hydration which may lead to lipid exchange with the SC when applied on the surface of the skin (26). On topical application of NLCs, the ordered lipid structures form a thin film over the skin surface leading to higher occlusion and hydrating effects which results in swelling and opening of SC, leading to higher drug penetration. This is supported by our results of present study for CXBN formulations, where Cxb was detected only in SC and epidermis after 2 h of topical application. However, after 6 h of permeation, Cxb was found in SC, epidermis and dermis which was further increased over a period of 24

h. Similar results were reported for fluorescent dye (DID) encapsulated NLCs and NLCs modified with TAT (3). However, the fluorescence intensity for NLCs modified with TAT was significantly higher than unmodified NLCs as a function of time (3). This could be because of the deposition of TAT modified NLCs in SC during initial period of time, followed by permeation through SC, hair follicles and furrows from where they act as a reservoir (27). The NLCs follow the shunt route easily, as particles below 300 nm in size can readily penetrate and accumulate in the hair follicles (3). However, the follicular route covers very small portion of the total skin permeation pathways. Therefore the objective of the present study was to enhance the permeation of the Cxb into the deep epidermis from other routes in addition to follicular route.

In vitro skin permeation results strongly suggest the importance of the CPPs in the skin retention of Cxb from the NLCs. NLCs modified with CPPs showed significantly higher retention of Cxb for all time points ($p<0.001$) compared to unmodified and YKA modified NLCs in different skin layers. The increased levels of Cxb in different layers of the skin after surface modification of NLCs with CPPs can be explained by the combined effects of occlusion by NLCs and translocation ability of CPPs. The CPPs may join the SC lipid bilayers in the intercellular regions leading to an overall increase in the membrane permeability of the applied Cxb (28). Different arginine chain length containing peptides showed a considerable difference in the transduction efficiency and Cxb delivery into the skin. Among all CPPs, R_{11} exhibited maximum internalization and accumulation of Cxb in deep skin layers. This might be because of the optimum positive charge of the polyarginine peptide (R_{11}) (4) or destabilization and formation of a pore in the SC lipids (29)-(30) which augments transport of NLCs encapsulated drug across the skin depths. Similar results were reported for reversed hexagonal lyotropic liquid crystals ($H_{II}LC$) of sodium diclofenac combined with various CPPs. In this reported study among various CPPs, nona-arginine (NONA) resulted in 2.2 fold increase in total amount of sodium diclofenac that diffused through the porcine skin (31-32). These results are in agreement with our skin permeation studies performed for CXBN modified with R_{11}, signifying highest translocation ability of R_{11} compared to other polyarginine peptides. However, the Cxb retention in the skin for CXBN-R_{15} was significantly less ($p<0.001$) than CXBN-R_{11}, possibly due to super saturation or hindrance effect from longer arginine chain length. Overall, the levels of Cxb in all three skin layers from CXBN-R_{11} were significantly less ($p<0.001$) than TAT and other polyarginines. Thus, based on in vitro skin permeation studies, CXBN-R_{11} was selected for further in vivo investigation of pharmacokinetic parameters of Cxb in normal skin and expression of biomarkers in the damaged skin along with therapeutic response in ACD model.

Dermal MD is an effective technique for the evaluation of drug absorption into the skin following topical application of formulations. Indeed, many reports are available on detection of unbound fraction of the NSAIDs at the target site from topical formulations using MD in rats, pigs and humans (33-34). Therefore, the dermal MD technique was adopted to evaluate the Cxb levels in the skin on unocclusive topical application of CXBS, CXBN, CXBN-R_{11} and CXBN YKA. Such information is particularly useful to predict pharmacokinetic and pharmacodynamic properties like lag time, AUC or acting duration of the Cxb from nanoparticles. For dermal pharmacokinetic study, we have selected 24 h permeation time since MD catheters are reported to be functional for 24 h period and thus it is capable of producing relevant data which can be correlated with end point biopsy data (35). Furthermore, our in vitro skin permeation results suggested that the Cxb retention in the skin for unmodified and CPP modified NLCs was 4.4 times higher at 24 h than 12 h. Calibration methods in MD are important when quantitative measurement of the extracellular fluid concentrations of the drug is desired. Here we have selected commonly used in vivo reterodialysis method for recovery studies, as drug recovery from tissue to

perfusate and across the probe membrane is very important to know prior to the in vivo experiments. The recovery rate of Cxb suggested that approximately 80% drug can be recovered from the probes when inserted into the skin. The observed Tmax for CXBS was 4 h while the average Tmax for NLC based formulations was 15 h, this proves the hypothesis that NLCs form an occlusive layer on the skin surface and acts as a drug reservoir within the upper layers of the SC and from there drug is released in a controlled fashion. Similarly, the half-life of brucine liposomes was 2.6 times higher than brucine solution (36). The AUC measured by dermal MD represents the total amount of drug which penetrated through SC, followed by epidermis and finally diffused into dermis after 24 h (12). Therefore two pharmacokinetic parameters namely, $AUC_{0\text{-}24h}$ and Cmax were assessed which showed considerably higher values ($p<0.001$) for CXBN-R_{11} suggesting the ability of R_{11} to deliver significant amounts of Cxb in the dermis. In addition, the in vivo MD data complements the in vitro permeation data, where higher amounts of Cxb were detected in all cutaneous layers at the end of 24 h for CXBNR_{11}.

MD has proved to be an effective technique to evaluate endogenous substances (17-18, 35). In response to topical application of allergens or irritants, increased expression of arachidonic acid, several pro-inflammatory and inflammatory markers including IL-6 and PGE_2 are found in the rat skin (17-18). The expression of PGE_2 reflects the intensity of skin irritation and Shinkai et al demonstrated that transdermal patch can deliver ketoprofen in sufficient amount to inhibit PGE_2 production in rat and pig skin (33-34). Several other studies have also recognized that the inducible enzyme COX-2 and its associated production of PGE_2 from arachidonic acid play an important role in initiation of inflammation (18). For the dermal irritation study, xylene was applied after 2 h of probe insertion (equilibration period), which was found to be optimal time to minimize the needle induced trauma. Topical exposure of xylene for 2 h significantly ($p<0.001$) increased the PGE_2 levels compared to untreated control (Fig. 7). PGE_2 levels declined gradually with time suggesting that the expression of PGE_2 is dependent on the xylene exposure time. However, pre-treatment of exposure site with CXBS, CXBN, CXBN-R_{11} and CXBN-YKA showed different levels of PGE_2 compared to untreated control. The pre-treatment with CXBNR_{11} showed significantly lower levels ($p<0.001$) of PGE_2 even after initial exposure of xylene. This suggests that CXBN-R_{11} can deliver sufficient amount of Cxb to inhibit the PGE_2 production in the skin compared to other formulations. These results are in agreement with the observation of Fulzele et al, where Cxb released from solution blocked the release of PGE_2 and substance P following JP-8 exposure (18). In rats, prostaniods activity appears in sequential relationship to other mediators of inflammation. The first step involves the release of histamine; the second step is associated with kinin activity; followed by third step with prostaglandin activity and second phase of histamine activity. Further, prostaglandins are recognized to participate in the inflammation cascade but do not appear to be an initial mediator. Therefore to further support our PGE_2 study we have studied the effect of pre-treatment with Cxb formulations on the expression of IL-6.

IL-6 is a secondary pro-inflammatory cytokine and is produced by stimulation of several other pathways like, interlukin-1 alpha (IL-1α), tumor necrosis factor-alpha (TNF-α), IL-17A and PGE_2 (17, 37-39). Langerhans cells in response to an irritant chemical result in production of IL-6 and several other inflammatory and pro-inflammatory mediators (37). The production of IL-6 is dependent on chemical insult, duration and irritation intensity. IL-6 levels increase transiently and return to normal after resolution of insult (40). However, the present study showed that after occlusive exposure of xylene for 2 h, the levels of IL-6 were significantly high for 5 h, even after removal of chemical exposure (only xylene treated samples, Fig. 8). These results are in agreement with our previous findings where the exposure of aliphatic hydrocarbons resulted in high levels of IL-6 even after 5 h from the removal of chemicals (17). In contrast to PGE_2, CXBN R_{11} pre-treated skin samples showed

elevated levels of IL-6 during xylene exposure. After removal of xylene, CXBN-R_{11} pre-treated skin showed a very low level of IL-6 expression which was significantly less ($p<0.001$) compared to CXBS, CXBN and CXBN-YKA. These results are in agreement with the in vitro skin permeation and in vivo pharmacokinetic studies and verify that the surface modification of CXBN with R_{11} is responsible for the increase in the skin permeation of Cxb along with reduced PGE_2 and IL-6 levels in the skin.

Further the effect of CXBN was investigated in an in vivo ACD model, where the reduction in ear thickness was evaluated as a response from different treatments. Acute inflammation is characterized by classical symptoms such as heat, redness, swelling and pain. Edema (swelling) is therefore a good measure of inflammation induced by phlogistic agents such as DNFB. The anti-ACD response for CXBN-R_{11} was significantly higher ($p<0.001$) than CXBS, CXBN and CXBNYKA for all the time points. The reduction in ear swelling by CXBN-R_{11} formulation was comparable to dexamethasone. Present study demonstrates that the results of in vitro skin retention and in vivo MD are correlated with the in vivo anti-inflammatory response of CXBNR_{11} in ACD mouse model. The response of ACD by Cxb formulations along with dexamethasone and control were further characterized by cutaneous histological examination. The reduction in ear thickness was observed for all Cxb treated mice ears compare to untreated control but the levels of reduction in ear swelling was observed to be different for different CxB formulations. CXBN-R_{11} topical treatment of sensitized mice after DNFB challenge resulted in reduction of both cutaneous edema and in the number of leukocytes infiltrating into the skin compared to CXBS, CXBN and CXBN-YKA. These results indicate that incorporating Cxb in NLC-R_{11} formulation facilitated diffusion of Cxb through skin layers.

CONCLUSION

Our studies demonstrate that the NLCs modified with R_{11} significantly improve the retention of Cxb in the skin layers as a function of time. This could be because of the positive charge and translocation ability of R_{11}. Further, dermal microdialysis can be successfully used to investigate the pharmacokinetic parameters and expression of inflammatory biomarkers like PGE_2 and IL-6 on topical application of surface modified and unmodified NLCs. The pre-treatment of CXBN-R_{11} was responsible for the increase in the skin permeation of Cxb and thus decrease in the PGE_2 and IL-6 levels during the skin inflammation induced by topical application of xylene, an irritant chemical. This further resulted in reduction of ear thickness and inflammation associated with an in vivo ACD model, suggesting the potential of R_{11} modified NLCs to treat various skin diseases and disorders like contact dermatitis, psoriasis and skin cancer where delivery of drug is required to be delivered in the deep skin layers.

Acknowledgments

This project was supported by the National Center for Research Resources and the National Institute of Minority Health and Health Disparities of the National Institutes of Health through Grant Number 8 G12 MD007582-28 and 2 G12 RR003020.

ABBREVIATIONS

NLC	Nano structured lipid carrier
Cxb	Celecoxib
CXBN	Cxb encapsulated NLCs

TAT	Trans-acting activator of transcription
CXBN-TAT	TAT coated CXBN
CXBN-R_8	Polyarginine-8 (R_8) coated CXBN
CXBN-R_{11}	Polyarginine-11 (R_{11}) coated CXBN
CXBN-R_{15}	Polyarginine-11 (R_{15}) coated CXBN
CXBN-YKA	YKA coated CXBN
CXBS	Celecoxib-solution
DOGS-NTA-Ni	1,2-dioleoyl-*sn*-glycero-3-[(*N*-(5-amino-1-carboxypentyl) imidodiacetic acid) succinyl nickel salt]
CPP	Cell Penetrating Peptide
MD	Microdialysis
PGE_2	Prostaglandin E2
IL-6	Interleukin-6
ACD	Allergic contact dermatitis

REFERENCES

1. Jensen LB, Petersson K, Nielsen HM. In vitro penetration properties of solid lipid nanoparticles in intact and barrier-impaired skin. Eur J Pharm Biopharm. 2011; 79:68–75. [PubMed: 21664463]
2. Baroli B. Penetration of nanoparticles and nanomaterials in the skin: fiction or reality? J Pharm Sci. 2010; 99:21–50. [PubMed: 19670463]
3. Patlolla RR, Desai PR, Belay K, Singh MS. Translocation of cell penetrating peptide engrafted nanoparticles across skin layers. Biomaterials. 2010; 31:5598–607. [PubMed: 20413152]
4. Desai PR, Patlolla RR, Singh M. Interaction of nanoparticles and cell-penetrating peptides with skin for transdermal drug delivery. Mol Membr Biol. 2010; 27:247–59. [PubMed: 21028936]
5. Mitchell DJ, Kim DT, Steinman L, Fathman CG, Rothbard JB. Polyarginine enters cells more efficiently than other polycationic homopolymers. J Pept Res. 2000; 56:318–25. [PubMed: 11095185]
6. Futaki S, Nakase I, Suzuki T, Youjun Z, Sugiura Y. Translocation of branched-chain arginine peptides through cell membranes: flexibility in the spatial disposition of positive charges in membrane-permeable peptides. Biochemistry. 2002; 41:7925–30. [PubMed: 12069581]
7. Futaki S, Suzuki T, Ohashi W, Yagami T, Tanaka S, Ueda K, et al. Arginine-rich peptides. An abundant source of membrane-permeable peptides having potential as carriers for intracellular protein delivery. J Biol Chem. 2001; 276:5836–40. [PubMed: 11084031]
8. Mathy FX, Ntivunwa D, Verbeeck RK, Preat V. Fluconazole distribution in rat dermis following intravenous and topical application: a microdialysis study. J Pharm Sci. 2005; 94:770–80. [PubMed: 15729707]
9. Groth L, Serup J. Cutaneous microdialysis in man: effects of needle insertion trauma and anaesthesia on skin perfusion, erythema and skin thickness. Acta Derm Venereol. 1998; 78:5–9. [PubMed: 9498017]
10. Mathy FX, Denet AR, Vroman B, Clarys P, Barel A, Verbeeck RK, et al. In vivo tolerance assessment of skin after insertion of subcutaneous and cutaneous microdialysis probes in the rat. Skin Pharmacol Appl Skin Physiol. 2003; 16:18–27. [PubMed: 12566825]
11. Holmgaard R, Nielsen JB, Benfeldt E. Microdialysis sampling for investigations of bioavailability and bioequivalence of topically administered drugs: current state and future perspectives. Skin Pharmacol Physiol. 2010; 23:225–43. [PubMed: 20484965]

12. Benfeldt E, Hansen SH, Volund A, Menne T, Shah VP. Bioequivalence of topical formulations in humans: evaluation by dermal microdialysis sampling and the dermatopharmacokinetic method. J Invest Dermatol. 2007; 127:170–8. [PubMed: 16874309]
13. Stenken JA, Church MK, Gill CA, Clough GF. How minimally invasive is microdialysis sampling? A cautionary note for cytokine collection in human skin and other clinical studies. AAPS J. 2010; 12:73–8. [PubMed: 19950008]
14. Kreilgaard M. Assessment of cutaneous drug delivery using microdialysis. Adv Drug Deliv Rev. 2002; 54:S99–121. [PubMed: 12460718]
15. Salgo R, Thaci D, Boehncke S, Diehl S, Hofmann M, Boehncke WH. Microdialysis documents changes in the micromilieu of psoriatic plaques under continuous systemic therapy. Exp Dermatol. 2011; 20:130–3. [PubMed: 21255092]
16. Shakeel F, Baboota S, Ahuja A, Ali J, Shafiq S. Skin permeation mechanism and bioavailability enhancement of celecoxib from transdermally applied nanoemulsion. J Nanobiotechnology. 2008; 6:8. [PubMed: 18613981]
17. Patlolla RR, Mallampati R, Fulzele SV, Babu RJ, Singh M. Dermal microdialysis of inflammatory markers induced by aliphatic hydrocarbons in rats. Toxicol Lett. 2009; 185:168–74. [PubMed: 19152832]
18. Fulzele SV, Babu RJ, Ahaghotu E, Singh M. Estimation of proinflammatory biomarkers of skin irritation by dermal microdialysis following exposure with irritant chemicals. Toxicology. 2007; 237:77–88. [PubMed: 17574719]
19. Souto EB, Wissing SA, Barbosa CM, Muller RH. Development of a controlled release formulation based on SLN and NLC for topical clotrimazole delivery. Int J Pharm. 2004; 278:71–7. [PubMed: 15158950]
20. Babu RJ, Kanikkannan N, Kikwai L, Ortega C, Andega S, Ball K, et al. The influence of various methods of cold storage of skin on the permeation of melatonin and nimesulide. J Control Release. 2003; 86:49–57. [PubMed: 12490372]
21. Kearney JN. Guidelines on processing and clinical use of skin allografts. Clin Dermatol. 2005; 23:357–64. [PubMed: 16023931]
22. Patlolla RR, Chougule M, Patel AR, Jackson T, Tata PN, Singh M. Formulation, characterization and pulmonary deposition of nebulized celecoxib encapsulated nanostructured lipid carriers. J Control Release. 2010; 144:233–41. [PubMed: 20153385]
23. Shah¥ P, Desai¥ P, Channer D, Singh M. Enhanced skin permeation using polyarginine modified nanostructured lipid carriers. J Control Release. 2012 In Press (¥ Contributed equally).
24. Shah P, Desai P, Patel A, Singh M. Skin permeating nanogel for the cutaneous co-delivery of two anti-inflammatory drugs. Biomaterials. 2012; 33:1607–17. [PubMed: 22118820]
25. Shah PP, Desai P, Singh M. Effect of oleic acid modified polymeric bilayered nanoparticles on percutaneous delivery of spantide II and ketoprofen. J Control Release. 2012; 158:336–345. [PubMed: 22134117]
26. Schafer-Korting M, Mehnert W, Korting HC. Lipid nanoparticles for improved topical application of drugs for skin diseases. Adv Drug Deliv Rev. 2007; 59:427–43. [PubMed: 17544165]
27. Prow TW, Grice JE, Lin LL, Faye R, Butler M, Becker W, et al. Nanoparticles and microparticles for skin drug delivery. Adv Drug Deliv Rev. 2011; 63:470–91. [PubMed: 21315122]
28. Fang JY, Fang CL, Liu CH, Su YH. Lipid nanoparticles as vehicles for topical psoralen delivery: Solid lipid nanoparticles (SLN) versus nanostructured lipid carriers (NLC). Eur J Pharm Biopharm. 2008; 70:633–40. [PubMed: 18577447]
29. Lopes LB, Furnish E, Komalavilas P, Seal BL, Panitch A, Bentley MV, et al. Enhanced skin penetration of P20 phosphopeptide using protein transduction domains. Eur J Pharm Biopharm. 2008; 68:441–5. [PubMed: 18035527]
30. Uchida T KT, Takashima Y, Okada H. Development of an efficient transdermal delivery system of small interfering RNA using functional peptides, Tat and AT-1002. Chem Pharm Bull (Tokyo). 2011; 59:196–201. [PubMed: 21297299]
31. Cohen-Avrahami M, Libster D, Aserin A, Garti N. Sodium diclofenac and cell-penetrating peptides embedded in H(II) mesophases: physical characterization and delivery. J Phys Chem B. 2011; 115:10189–97. [PubMed: 21749044]

32. Cohen-Avrahami M, Aserin A, Garti N. H(II) mesophase and peptide cell-penetrating enhancers for improved transdermal delivery of sodium diclofenac. Colloids Surf B Biointerfaces. 2010; 77:131–8. [PubMed: 20189781]
33. Shinkai N, Korenaga K, Takizawa H, Mizu H, Yamauchi H. Percutaneous penetration of felbinac after application of transdermal patches: relationship with pharmacological effects in rats. J Pharm Pharmacol. 2008; 60:71–6. [PubMed: 18088507]
34. Shinkai N, Korenaga K, Okumura Y, Mizu H, Yamauchi H. Microdialysis assessment of percutaneous penetration of ketoprofen after transdermal administration to hairless rats and domestic pigs. Eur J Pharm Biopharm. 2011; 78:415–21. [PubMed: 21397690]
35. Sjogren F, Anderson CD. Are cutaneous microdialysis cytokine findings supported by end point biopsy immunohistochemistry findings? AAPS J. 2010; 12:741–9. [PubMed: 20967522]
36. Yang BC, Chu ZF, Zhu S, Wang LJ, Feng YH, Li FH, et al. Study of pharmacokinetics and tissue distribution of liposomal brucine for dermal administration. Int J Nanomedicine. 2011; 6:1109–16. [PubMed: 21698079]
37. Eberle T, Doganci B, Kramer H, Fechir M, Wagner I, Sommer C, et al. Mechanical but not painful electrical stimuli trigger TNF alpha release in human skin. Exp Neurol. 2010; 221:246–50. [PubMed: 19931249]
38. Zhang F, Koyama Y, Sanuki R, Mitsui N, Suzuki N, Kimura A, et al. IL-17A stimulates the expression of inflammatory cytokines via celecoxib-blocked prostaglandin in MC3T3-E1 cells. Arch Oral Biol. 2010; 55:679–88. [PubMed: 20630498]
39. Davis TW, Zweifel BS, O'Neal JM, Heuvelman DM, Abegg AL, Hendrich TO, et al. Inhibition of cyclooxygenase-2 by celecoxib reverses tumor-induced wasting. J Pharmacol Exp Ther. 2004; 308:929–34. [PubMed: 14711936]
40. Hirano T. Interleukin-6 and its relation to inflammation and disease. Clin Immunol Immunopathol. 1992; 62:S60–5. [PubMed: 1728989]

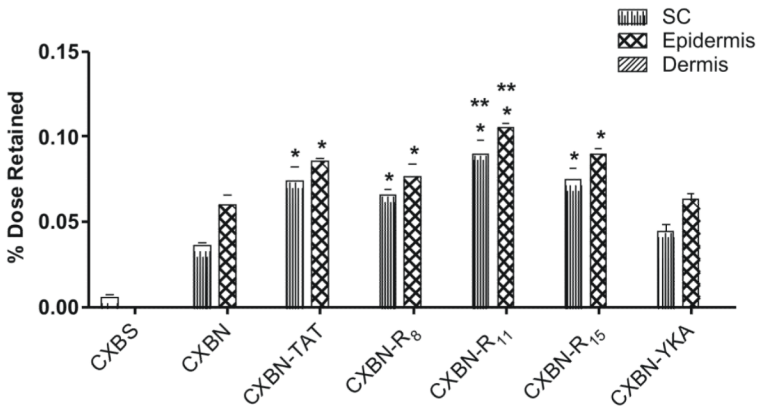

Fig. 1.

In vitro skin permeation of surface modified and unmodified CXBN for 2 h: Effect of different CPPs on the skin permeation of Cxb encapsulated NLC formulations. In vitro skin permeation studies were carried out in full thickness rat skin using Franz diffusion cells and after 2 h of application, the skin was collected and processed as described in methods section. Data represent mean ± SD, n=4, significance CPP engrafted CXBN against CXBS, CXBN and CXBNYKA, * $p<0.001$ and significance CXBN-R_{11} against CXBN-TAT, CXBN-R8 and CXBN-R15, ** $p<0.001$.

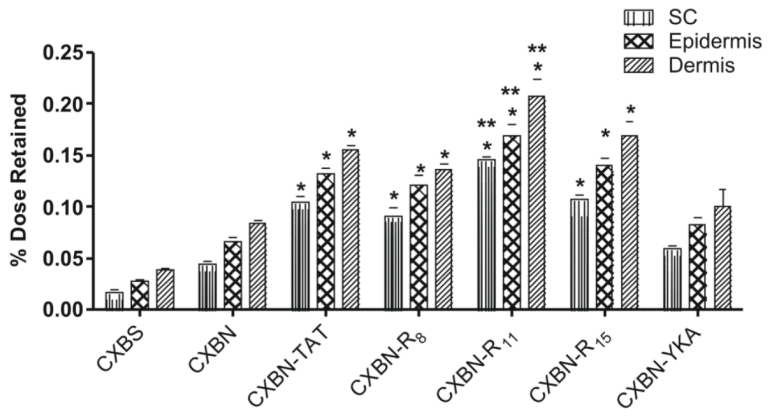

Fig. 2.

In vitro skin permeation of surface modified and unmodified CXBN for 6 h: Effect of different CPPs on the skin permeation of Cxb encapsulated NLC formulations. In vitro skin permeation studies were carried out in full thickness rat skin using Franz diffusion cells and after 6 h of application, the skin was collected and processed as described in methods section. Data represent mean ± SD, n=4, significance CPP engrafted CXBN against CXBS, CXBN and CXBNYKA, * $p<0.001$ and significance CXBN-R_{11} against CXBN-TAT, CXBN-R8 and CXBN-R15, ** $p<0.001$.

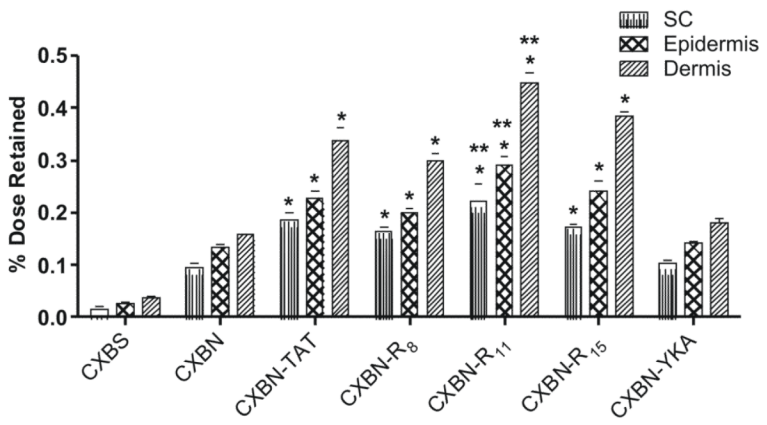

Fig. 3.

In vitro skin permeation of surface modified and unmodified CXBN for 12 h: Effect of different CPPs on the skin permeation of Cxb encapsulated NLC formulations. In vitro skin permeation studies were carried out in full thickness rat skin using Franz diffusion cells and after 12 h of application, the skin was collected and processed as described in methods section. Data represent mean ± SD, n=4, significance CPP engrafted CXBN against CXBS, CXBN and CXBNYKA, * $p<0.001$ and significance CXBN-R_{11} against CXBN-TAT, CXBN-R8 and CXBN-R15, ** $p<0.001$.

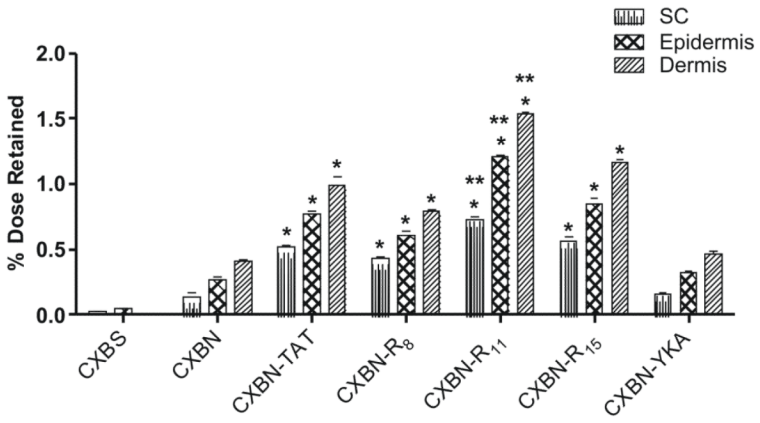

Fig. 4.

In vitro skin permeation of surface modified and unmodified CXBN for 24 h: Effect of different CPPs on the skin permeation of Cxb encapsulated NLC formulations. In vitro skin permeation studies were carried out in full thickness rat skin using Franz diffusion cells and after 24 h of application, the skin was collected and processed as described in methods section. Data represent mean ± SD, n=4, significance CPP engrafted CXBN against CXBS, CXBN and CXBN YKA, * $p<0.001$ and significance CXBN-R_{11} against CXBN-TAT, CXBN-R8 and CXBN-R15, ** $p<0.001$.

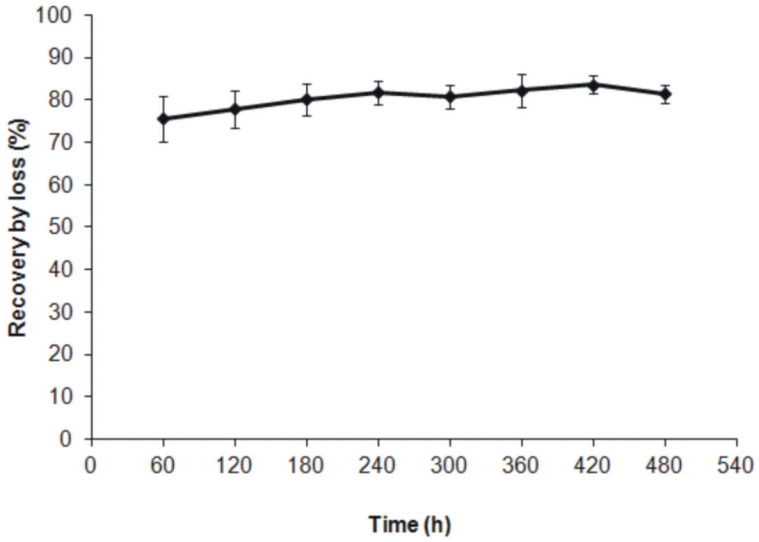

Fig. 5.

Assessment of loss of Cxb from MD probes using in vivo retrodialysis on hair less rats. Data represent mean ± SD, n=4.

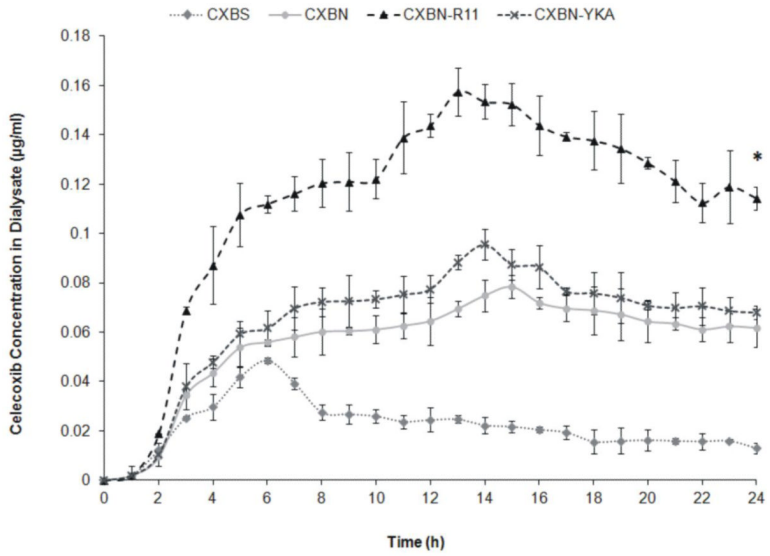

Fig. 6.

Concentration - time profiles for Cxb (μg/ml) in the skin when applied in a form of CXBS, modified and unmodified CXBN. The amount of Cxb in MD dialysate assessed every hour upto 24 h for various Cxb formulations. Data represent mean ± SD, n=4, significance CXBN-R_{11} against CXBS, CXBN and CXBN-YKA, * $p<0.001$.

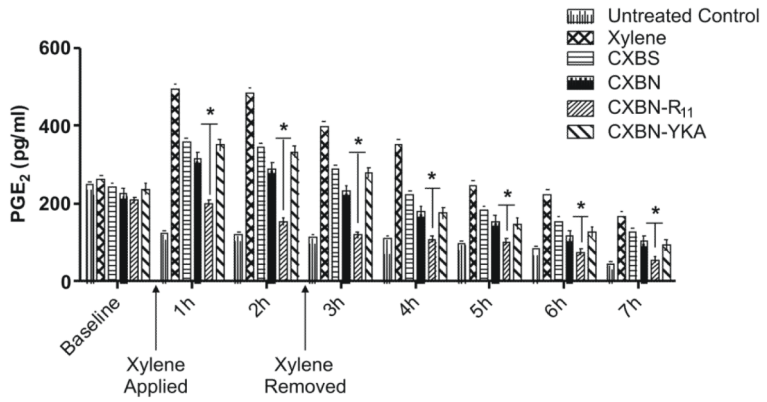

Fig. 7.

Mean concentration of PGE_2 (pg/ml) following pre-treatment with Cxb formulations, insertion of the probes, topical application of irritant chemical (xylene) and 5 h after removal of the chemical. The effect of pre-treatment (16 h) with surface modified and unmodified CXBN and CXBS was evaluated for the expression of PGE_2 in dialysate. Data represent mean ± SD, n=4, significance CXBN-R_{11} against CXBS, CXBN and CXBN-YKA, * $p<0.001$.

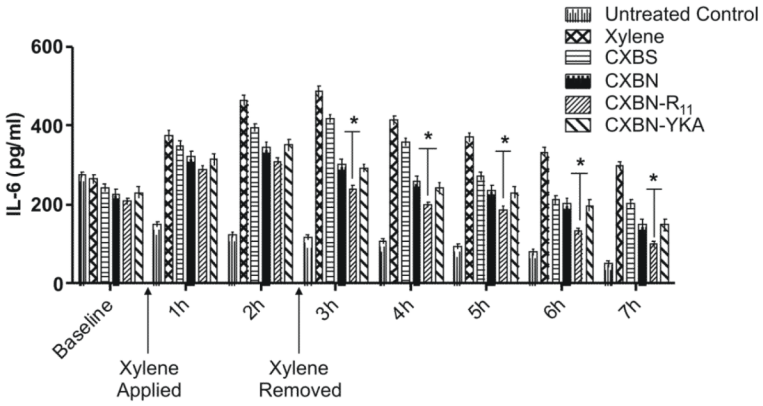

Fig. 8.

Mean concentration of IL-6 (pg/ml) following pre-treatment of Cxb formulations, insertion of the probes, topical application of irritant chemical (xylene) and 5 h after removal of the chemical. The effect of pre-treatment (16 h) with surface modified and unmodified CXBN and CXBS was evaluated for the expression of IL-6 in dialysate. Data represent mean ± SD, n=4, significance CXBN-R_{11} against CXBS, CXBN and CXBN-YKA, * $p<0.001$.

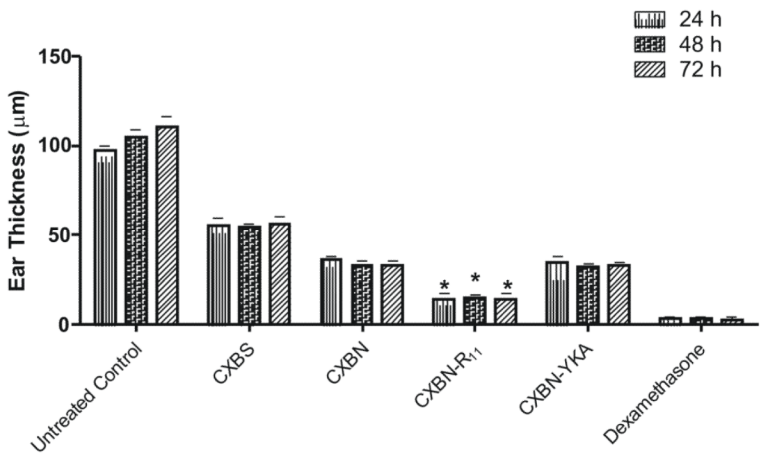

Fig. 9.

Effect of CXBS, surface modified and unmodified nanoparticles containing Cxb on the reduction of ACD in C57/BL mice ears. Data represent mean ± SD, n=4, significance CXBN-R_{11} against CXBS, CXBN and CXBN-YKA, * $p<0.001$.

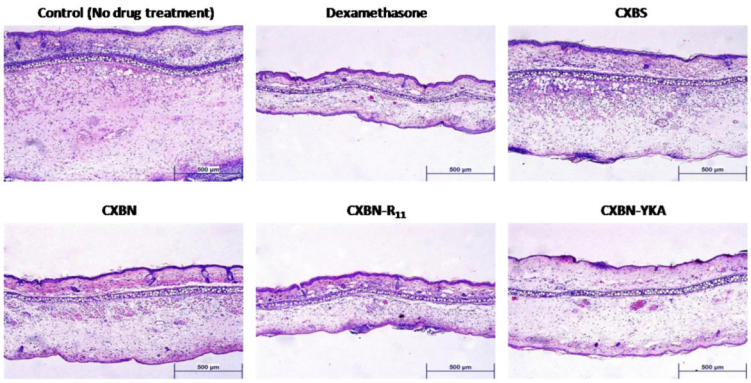

Fig. 10.

H&E staining of inflammation induced by topical application of DNFB, and after 72 h treatment CXBS, CXBN, CXBN-R_{11}, CABN-YKA and a positive control, dexamethasone.

Table I

In vitro recovery of Cxb, PGE_2 and IL-6 at the end of 240 min for five different flow rates. Data represent mean ± SD, n=4.

Substance	Flow Rate				
	0.5 μl/min	**1 μl/min**	**2 μl/min**	**3 μl/min**	**4 μl/min**
Cxb	57.48 ± 0.76	55.93 ± 0.82	55.07 ± 0.82	51.28 ± 0.77	45.16 ± 1.74
PGE_2	37.53 ± 1.2	35.56 ± 0.52	33.15 ± 0.71	34.37 ± 0.9	34.81 ± 0.49
IL-6	16.17 ± 0.96	12.01 ± 0.24	9.82 ± 1.12	5.51 ± 0.37	2.09 ± 0.07